

## Secondary interactions in the crystal structures of three 1,2,4,5-tetrakis(bromomethyl)-3,6-bis(2-alkoxy)benzenes

Christophe M.L. Vande Velde<sup>a,\*</sup>, Matthias Zeller<sup>b</sup>, Vladimir A. Azov<sup>c,\*</sup>

<sup>a</sup> Karel de Grote University College, Department of Applied Engineering, Salesianenlaan 30, 2660 Antwerp, Belgium

<sup>b</sup> Youngstown State University, One University Plaza, Youngstown, OH 44555-3663, USA

<sup>c</sup> Department of Chemistry, University of Bremen, Leobener Strasse NW 2C, D-28359 Bremen, Germany

### ARTICLE INFO

#### Article history:

Received 4 January 2012  
Received in revised form 16 February 2012  
Accepted 16 February 2012  
Available online 28 February 2012

#### Keywords:

Crystallography  
Non-covalent interactions  
Weak hydrogen bonds  
Halogen–halogen contacts  
Hirshfeld surfaces  
OpiX calculations

### ABSTRACT

Crystal structures of three 1,2,4,5-tetrakis(bromomethyl)-3,6-bis(2-alkoxy)benzenes **1–3** with different length and branching of alkyl chains are analyzed. X-ray structure determinations showed relatively undistorted molecular structures. Crystal packing is defined by networks of C–H···Br weak hydrogen bonds, short Br···Br contacts, and one particularly short C–H···π contact, although the major share of the cohesive energy of the structures is due to dispersion interactions.  $Z' = 2$  for **1** can be explained in terms of these interactions, which were shown to be stronger between the asymmetric pairs of molecules with the help of OpiX calculations. Surprisingly, the role of the oxygen atoms in intermolecular crystal packing is relatively small.

© 2012 Elsevier B.V. All rights reserved.

### 1. Introduction

The importance of the so called “weak interactions”, which include weak H-bonds, [1] halogen bonds, [2] and various types of interactions involving  $\pi$ -systems, [3] in shaping the formation of crystal lattices of organic compounds is now fully recognized. Deeper understanding of such weak interactions is of paramount importance for the directed creation of new organic materials for molecular electronics, photovoltaics, nonlinear optics, and other fields of modern materials science. Thus, investigations into the nature of weak H-bonds and halogen interactions are the topic of current interest and active research [4].

Herein we analyze the crystal packing of three 1,2,4,5-tetrakis(bromomethyl)-3,6-bis(alkoxy)benzenes **1–3** (Fig. 1) containing methyl, hexyl, and 2-ethylbutyl side chains. Due to the presence of four symmetrically disposed bromomethyl groups these kinds of derivatives were previously employed as intermediates in the synthesis of various molecular architectures, such as polyacenes, [5] tetrathiafulvalene cages, [6] molecular capsules, [7] and molecular tweezers. [8] Alkoxy groups were used either for improvement of solubility, or served as masked hydroxyl groups. Packing motifs for the three reported compounds show the presence of C–H···Br

weak hydrogen bonds and C–Br···Br contacts, as well as one C–H···π contact for the Me-derivative.

The analysis of intermolecular packing was performed with the help of Hirshfeld surfaces and fingerprint plots, which represent a novel approach to the investigation of intermolecular interactions in crystals [9]. Most commonly, the analysis of such interactions focuses on an examination of specific interatomic distances and angles, and short contact distances between atoms in neighboring molecules are considered to be an indication of important interactions. Use of Hirshfeld surfaces and fingerprint plots opens a possibility to obtain an unbiased picture of the complete supra-molecular environment over the whole molecular surface, as well as to handily define and evaluate the role of particular short contacts in a crystal structure.

### 2. Experimental

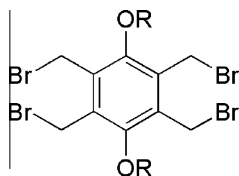
#### 2.1. Synthesis and crystallization

Compounds **1** [5a] and **2** [6b] were prepared as reported before. 1,2,4,5-Tetrakis(bromomethyl)-3,6-bis(2-ethylbutoxy)benzene was prepared from 1,4-dihydroxy-2,3,5,6-tetramethylbenzene in two steps.

*1,4-Bis(2-ethylbutoxy)-2,3,5,6-tetramethylbenzene.* To a solution of 1,4-dihydroxy-2,3,5,6-tetramethylbenzene (1.44 g, 8.71 mmol) in absolute DMF (20 mL), NaH (0.46 g, 19.2 mmol, washed with

\* Corresponding authors. Tel.: +32 3 613 19 41 (C.M.L. Vande Velde), tel.: +49 421 218 63126, fax: +49 421 218 63120 (V.A. Azov).

E-mail addresses: [Christophe.VandeVelde@KdG.be](mailto:Christophe.VandeVelde@KdG.be) (C.M.L. Vande Velde), [vazov@uni-bremen.de](mailto:vazov@uni-bremen.de) (V.A. Azov).



- 1, R = Me  
 2, R = *n*-C<sub>6</sub>H<sub>13</sub>  
 3, R = CH<sub>2</sub>CH(C<sub>2</sub>H<sub>5</sub>)<sub>2</sub>

Fig. 1. Molecular structures of the compounds 1–3.

hexane and dried before addition) was added in small portions at room temperature within 20 min. Then 1-bromo-2-ethylpropane (2.68 mL, 19.2 mmol) was added dropwise over a period of 10–15 min upon cooling with an ice bath. The reaction mixture was stirred for 3 h at 60 °C and then evaporated to dryness. The residue was purified by flash chromatography (FC, SiO<sub>2</sub>, PE/CH<sub>2</sub>Cl<sub>2</sub>, gradient 0–40%) yielding 1.19 g (3.56 mmol, 41%) of flake-like colorless crystals. *R*<sub>f</sub> = 0.42 (CH<sub>2</sub>Cl<sub>2</sub>/*n*-hexane, 2:3). Mp 52.5–53 °C. <sup>1</sup>H NMR (200 MHz, CDCl<sub>3</sub>): δ = 0.95 (t, 12H, *J* = 7.4 Hz), 1.40–1.73 (m, 10H), 2.15 (s, 12H), 3.52 (d, 4H, *J* = 5.6 Hz). <sup>13</sup>C NMR (50 MHz, CDCl<sub>3</sub>): δ = 11.49, 12.99, 23.44, 42.42, 75.35, 127.85, 151.83. HR-EI-MS (70 eV): *m/z* = 334.28674 (M<sup>+</sup>, C<sub>22</sub>H<sub>38</sub>O<sub>2</sub><sup>+</sup>, calcd. 334.28718).

1,2,4,5-Tetrakis(bromomethyl)-3,6-bis(2-ethylbutoxy)benzene 3. A mixture of 1,4-bis(2-ethylbutoxy)-2,3,5,6-tetramethylbenzene (1.10 g, 3.29 mmol), finely powdered *N*-bromosuccinimide (NBS, 2.46 g, 13.8 mmol), and dibenzoyl peroxide (40 mg, 0.164 mmol) was refluxed in 20 mL of carbon tetrachloride for 1.5 h. After checking the progress of the reaction by NMR an additional 0.5 eq. NBS and a spatula tip of dibenzoyl peroxide were added to the reaction mixture, which was refluxed for additional 1.5 h.

The mixture was cooled with an ice bath, the precipitate was filtered off, the organic phase was washed with Na<sub>2</sub>S<sub>2</sub>O<sub>3</sub> solution and brine, dried (Na<sub>2</sub>SO<sub>4</sub>), and evaporated to dryness. The residue was recrystallized from hexane/CH<sub>2</sub>Cl<sub>2</sub> to afford a first crop of the product. The mother liquor was evaporated to dryness, and the residue was purified by FC (SiO<sub>2</sub>, PE/CH<sub>2</sub>Cl<sub>2</sub>, gradient 0–15%). Total yield amounted to 1.70 g (2.61 mmol, 79%) of colorless crystals. *R*<sub>f</sub> = 0.35 (CH<sub>2</sub>Cl<sub>2</sub>/*n*-hexane, 1:5). Mp 148–150 °C. <sup>1</sup>H NMR (200 MHz, CDCl<sub>3</sub>): δ = 1.01 (t, 12H, *J* = 7.4 Hz), 1.50–1.67 (m, 8H), 1.84 (p, 2H, *J* = 6.0 Hz), 4.05 (d, 4H, *J* = 6.0 Hz), 4.76 ppm (s, 12H). <sup>13</sup>C NMR (50 MHz, CDCl<sub>3</sub>): δ = 11.47, 23.19, 23.47, 42.35, 77.69, 133.47, 153.63 ppm. HR-EI-MS (70 eV): *m/z* = 645.92745 (M<sup>+</sup>, C<sub>22</sub>H<sub>34</sub>Br<sub>4</sub>O<sub>2</sub><sup>+</sup>, calcd. 645.92922).

X-ray quality crystals were grown by slow evaporation of chloroform (1) or dioxane (2) solutions or by slow diffusion of hexane into a chloroform solution (3).

## 2.2. X-ray data collection and refinement

Crystals of suitable size were mounted on a Bruker platform three-circle goniometer with SMART APEX detector, and graphite-monochromated MoKα tube, and flash-cooled to 100 K. ω-Scans were collected. Data were reduced with the Bruker APEX2 [10] software and scaled and corrected for absorption effects using SADABS. The structures were solved by direct methods with the help of SIR92 [11], refinements were carried out by full-matrix least-square techniques using CRYSTALS [12]. All non-hydrogen atoms were refined anisotropically. The H atoms were located from a difference map and initially refined with soft restraints on the bond lengths and angles to regularize their geometry (C–H in the range 0.93–0.98 Å) and *U*<sub>iso</sub>(H) (in the range 1.2–1.5 times *U*<sub>eq</sub> of the parent atom), after which the positions were refined with riding constraints [13]. Crystal data together with collection and refinement details for compounds 1–3 are presented in Table 1.

Table 1  
 Crystal data, collection and refinement details for compounds 1 and 2.

	1	2	3
Formula	C <sub>12</sub> H <sub>14</sub> Br <sub>4</sub> O <sub>2</sub>	C <sub>22</sub> H <sub>34</sub> Br <sub>4</sub> O <sub>2</sub>	C <sub>22</sub> H <sub>34</sub> Br <sub>4</sub> O <sub>2</sub>
<i>M</i> <sub>r</sub>	509.86	650.12	650.12
Crystal system, space group	Triclinic, <i>P</i> $\bar{1}$	Monoclinic, <i>P</i> 2 <sub>1</sub> / <i>c</i>	Triclinic, <i>P</i> $\bar{1}$
<i>a</i> (Å)	9.4482(11)	11.9079 (17)	8.610 (3)
<i>b</i> (Å)	9.7673(14)	5.0428 (7)	8.776 (3)
<i>c</i> (Å)	10.0131(15)	20.687 (3)	9.557 (3)
α (°)	118.315(2)		74.914 (4)
β (°)	107.831(11)	102.470 (2)	64.397 (4)
γ (°)	96.19(3)		70.664 (4)
<i>V</i> (Å <sup>3</sup> )	738.3(2)	1212.9 (3)	608.6 (4)
<i>Z</i>	2	2	1
<i>D</i> <sub>calc</sub> (g cm <sup>-3</sup> )	2.293	1.780	1.774
μ (mm <sup>-1</sup> )	10.89	6.65	6.63
<i>F</i> (000)	484	644	322
Crystal color, habit	Colorless, block	Colorless, needle	Colorless, block
Crystal size (mm)	0.22 × 0.39 × 0.50	0.55 × 0.20 × 0.18	0.36 × 0.28 × 0.25
Temperature (K)	100	100	100
Radiation type, wavelength (Å)	Mo Kα, 0.71073	Mo Kα, 0.71073	Mo Kα, 0.71073
θ range (°)	2.4–31.3	1.8–31.3	2.4–31.3
Index range	–13 ≤ <i>h</i> ≤ 12 –14 ≤ <i>k</i> ≤ 12 0 ≤ <i>l</i> ≤ 14	–16 ≤ <i>h</i> ≤ 16 0 ≤ <i>k</i> ≤ 7 0 ≤ <i>l</i> ≤ 30	–10 ≤ <i>h</i> ≤ 12 –11 ≤ <i>k</i> ≤ 12 0 ≤ <i>l</i> ≤ 13
Absorption correction	Multi-scan, SADABS, Bruker APEX2 [10]		
<i>T</i> <sub>min</sub> , <i>T</i> <sub>max</sub>	0.343, 0.746	0.316, 0.746	0.565, 0.746
No. of reflections measured, independent, observed [ <i>I</i> > 2.0σ( <i>I</i> )]	7669, 4364, 3762	6734, 3574, 2883	9836, 3615, 3199
<i>R</i> <sub>int</sub>	0.028	0.034	0.022
No. of reflection, parameters, restraints	4364, 164, 0	3574, 127, 0	3615, 127, 0
<i>R</i> [ <i>F</i> <sup>2</sup> > 2σ( <i>F</i> <sup>2</sup> )], <i>wR</i> ( <i>F</i> <sup>2</sup> ), <i>S</i>	0.030, 0.073, 1.01	0.034, 0.092, 0.96	0.021, 0.055, 1.00
Δρ <sub>max</sub> , Δρ <sub>min</sub> (e Å <sup>-3</sup> )	1.42, –1.06	0.97, –1.08	1.19, –0.50

ORTEP diagrams were drawn using Ortep-3 for Windows [14]. Crystal structures were analyzed using the PLATON package [15] as well as with the help of Hirshfeld surfaces and fingerprint plots [9], prepared using Crystal Explorer 2.1 [16]. Packing diagrams were prepared with the help of Mercury v. 2.4.6 [17].

### 2.3. Hirshfeld surface analysis

Molecular Hirshfeld surfaces in crystal structures are based on the electron distribution calculated as the sum of spherical atom electron densities of a molecule [18]. The Hirshfeld surface enclosing a molecule is defined by points where the local density in the crystal equals twice the promolecular density of the single molecule. For each point on such an isosurface two distances are defined:  $d_e$ , the distance from the point to the nearest nucleus external to the surface, and  $d_i$ , the distance to the nearest nucleus internal to the surface. The normalized contact distance,  $d_{\text{norm}}$ , is a symmetric function based on both  $d_e$  and  $d_i$ , and the van der Waals (vdW) radii of atoms internal or external to the surface:

$$d_{\text{norm}} = (d_i - r_i^{\text{vdw}}) / r_i^{\text{vdw}} + (d_e - r_e^{\text{vdw}}) / r_e^{\text{vdw}}$$

The value of  $d_{\text{norm}}$  is negative/positive when intermolecular contacts are shorter/longer than vdW separations, enabling

identification of the regions of particular interest in relation to intermolecular interactions.

The combination of  $d_i$  and  $d_e$  in the form of a 2D fingerprint plot affords a concise summary of intermolecular contacts in the crystal [19]. Such plots are generated by binning of ( $d_i$ ,  $d_e$ ) pairs in intervals of 0.01 Å and coloring each bin (a single pixel on the plot) of the resulting 2D histogram as a function of the fraction of surface points in that bin. Resolved fingerprint plots can be efficiently used to identify particular close contacts in the crystal structure, such as H-bonds or halogen–halogen interactions.

Hirshfeld surfaces became a useful tool for the analysis of intermolecular interactions in crystals and were employed in studies of phenomena such as polymorphism [20], inclusion complexes [21], pressure-induced effects [20a,22], and others.

### 2.4. OPiX calculations

An electron density cube for the crystal geometry of **1** was calculated with Gaussian 03 [23] at the DFT/B3LYP/6-311G\* level. The electron density was used to evaluate packing energies using the PIXEL method as implemented in the program OPiX [24]. UNI force field calculations for **1–3** were performed with OPiX. For the OPiX calculations, the CIFs were modified so that they would contain

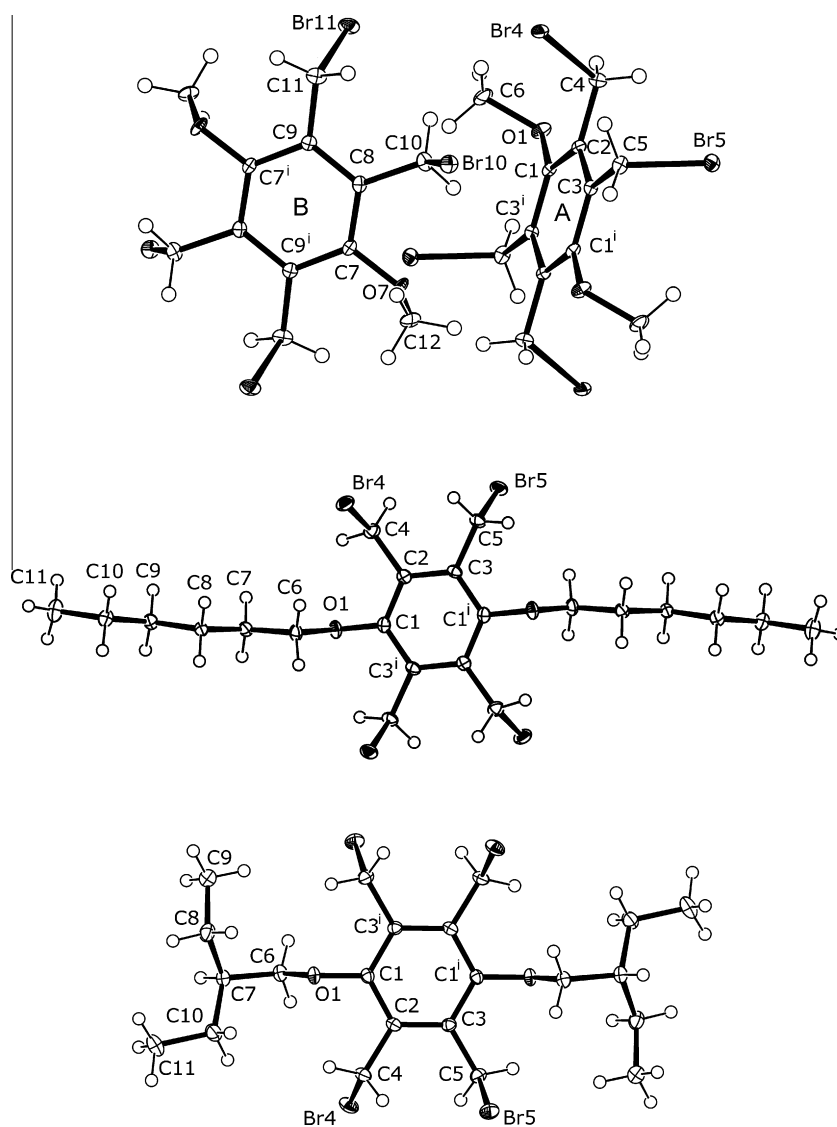


Fig. 2. ORTEP plots of **1–3**. Thermal ellipsoids are shown with 50% probability. For compound **1**, two asymmetric molecules are labeled as “A” and “B”.

whole molecules as opposed to symmetry unique half-molecules (removal of the  $-x$ ,  $-y$ ,  $-z$  operator and explicit entering of the corresponding coordinates), leading to a difference in symmetry operators between the results of the OpiX calculations and the crystal structure determinations. For **2**, also the origin was shifted by  $(-1/2, -1/2, -1/2)$ . The output from these calculations yields a total packing energy and a breakdown into component interactions. Each energy is further broken down into its Coulombic (electrostatic), polarization, dispersion and repulsion contributions [25].

### 3. Results and discussion

#### 3.1. Molecular structures

The molecular structures are shown in Fig. 2. Molecules of all three compounds crystallize on a center of symmetry. Compound **1** crystallizes in space group  $P\bar{1}$  with  $Z = 2$ , and has two symmetrically unrelated half molecules in the asymmetric unit. Both asymmetric molecules of **1** adopt almost identical conformations, in which differences in torsion angles for the corresponding substituents (OCH<sub>3</sub> and CH<sub>2</sub>Br groups) lie within 10°. Bond lengths and angles for the three compounds may be considered normal. The range of C–Br bond lengths is 1.972(2)–1.982(3) Å, whereas the aromatic C–C distances lie within the 1.395(4)–1.408(4) Å interval. Despite the 6-fold substitution, the benzene rings do not show any significant deviation from planarity. The highest ring torsion angles



Fig. 3. Network of short contacts shown on example of one asymmetric molecule of **1**. Similar contact patterns are observed in crystals of compounds **2** and **3**.

reach  $\pm 1.7(5)^\circ$  for one of the asymmetric molecules in the crystals of **1**; for the second molecule of **1**, as well as for the compounds **2** and **3** torsion angles do not exceed  $\pm 0.3(5)^\circ$ . Such relatively small deviations from planarity are in contrast with hexa(bromomethyl)benzene, for which torsion angles reach  $\pm 6^\circ$  [26].

In all three compounds, absolute C–C–Br torsion angles span from 76.5(3)° to 91.3(3)°, whereas C–C–O angles are in the range of 83.5(2)–91.7(2)°. The disposition of the six substituents is identical for **1–3**: two CH<sub>2</sub>Br groups surround an alkoxy substituent, all of them pointing in the same direction. Thus, two neighboring CH<sub>2</sub>Br groups are oppositely oriented, in contrast with 1,2,4,5-tetrakis(bromomethyl)benzene, which shows *syn* orientation for the two pairs of neighboring CH<sub>2</sub>Br groups [27]. This arrangement of the substituents in the dialkoxy derivatives leads to a network of short intramolecular C–H···Br and C–H···O contacts, some of which may be regarded as weak intramolecular C–H···Br hydrogen bonds [28] (Fig. 3). The contacts interconnecting CH<sub>2</sub>Br and OCH<sub>3</sub> groups occur slightly below the sum of van der Waals radii of the involved atoms [29] (2.94–3.06 Å), with C–H···Br angles of 142–147°, implying the hydrogen bonding character of the observed interaction according to accepted distance/angle criteria for crystalline substances [1a,b]. The C–H···Br contact distances between the neighboring CH<sub>2</sub>Br groups are even shorter (2.79–2.93 Å), but show rather unfavorable donor (129–136°) and acceptor (*ca.* 65°) directionalities. Intramolecular C–H···O contacts are shorter still, but unfavorable donor (102–110°) directionalities do not allow classifying them as weak H-bonds. Taking into account the inability of the CH<sub>2</sub>Br groups to find another more favorable spatial orientation due to congestion of the benzene substituents, such close contacts may be repulsive in nature.

#### 3.2. Crystal packing

The main interest of the study focuses on details of supramolecular packing of the compounds. The availability of several H-bonding sites per molecule together with relatively high molecular symmetry gave expectations for interesting intermolecular packing.

Compound **1** shows the most complex molecular arrangement with numerous short contacts between the neighboring molecules. For the analysis of short contacts, Hirshfeld surfaces mapped with  $d_{\text{norm}}$  (Fig. 4) as well as fingerprint plots mapped with different

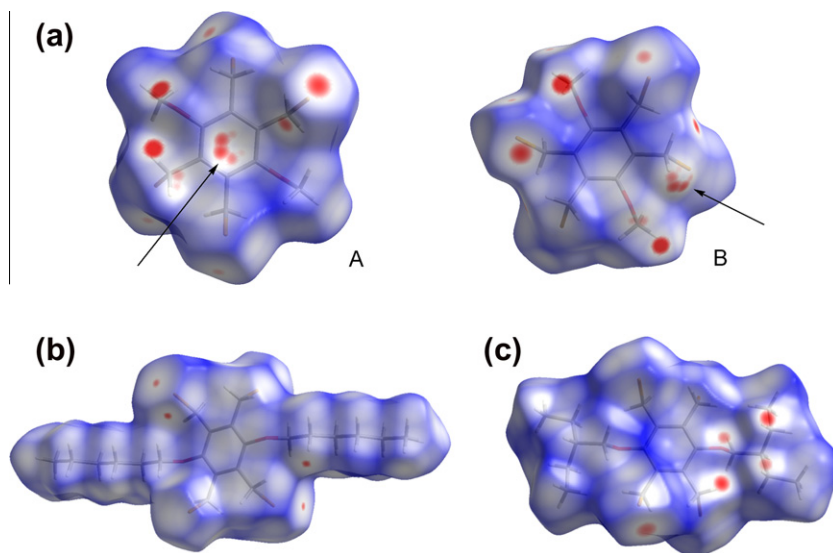
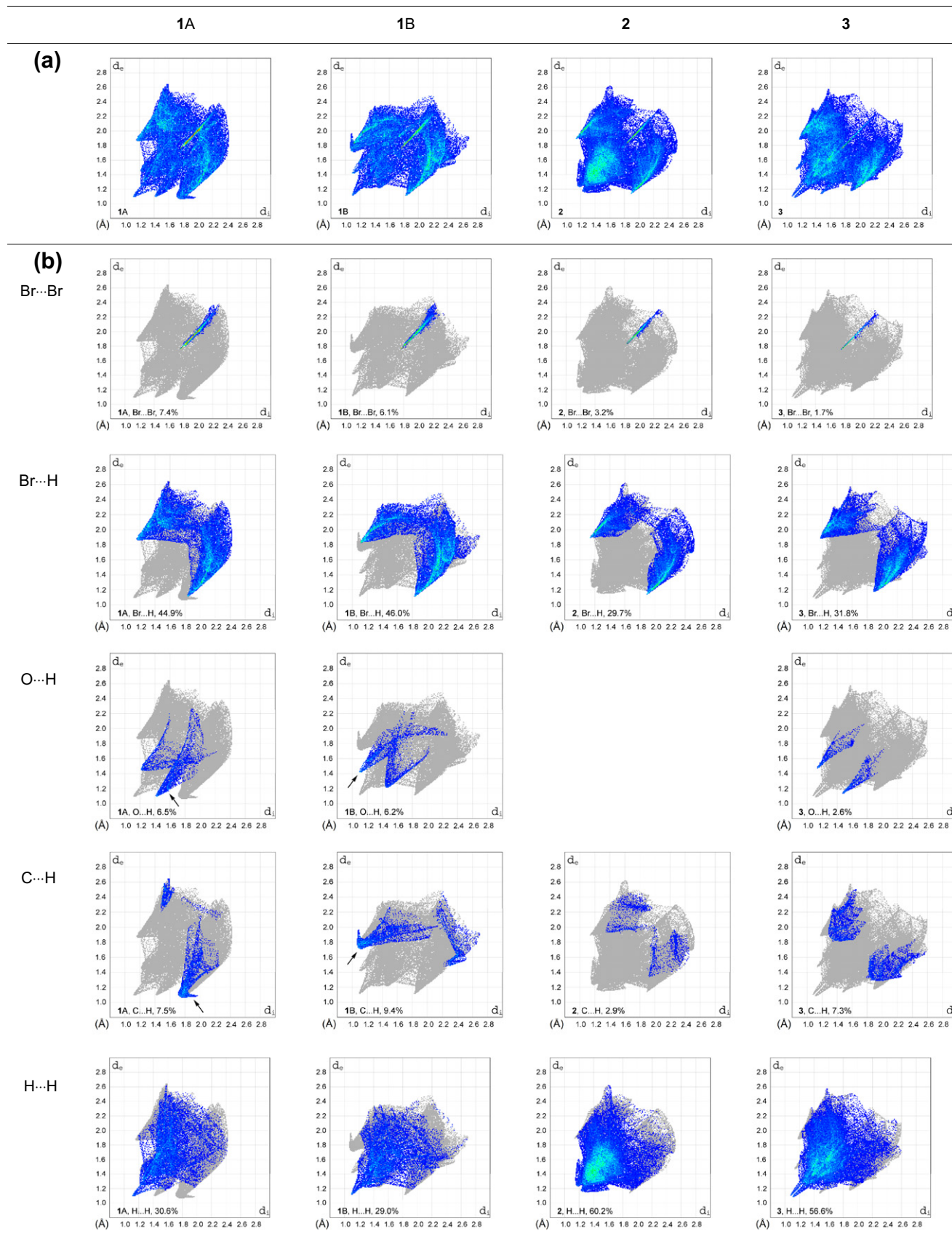
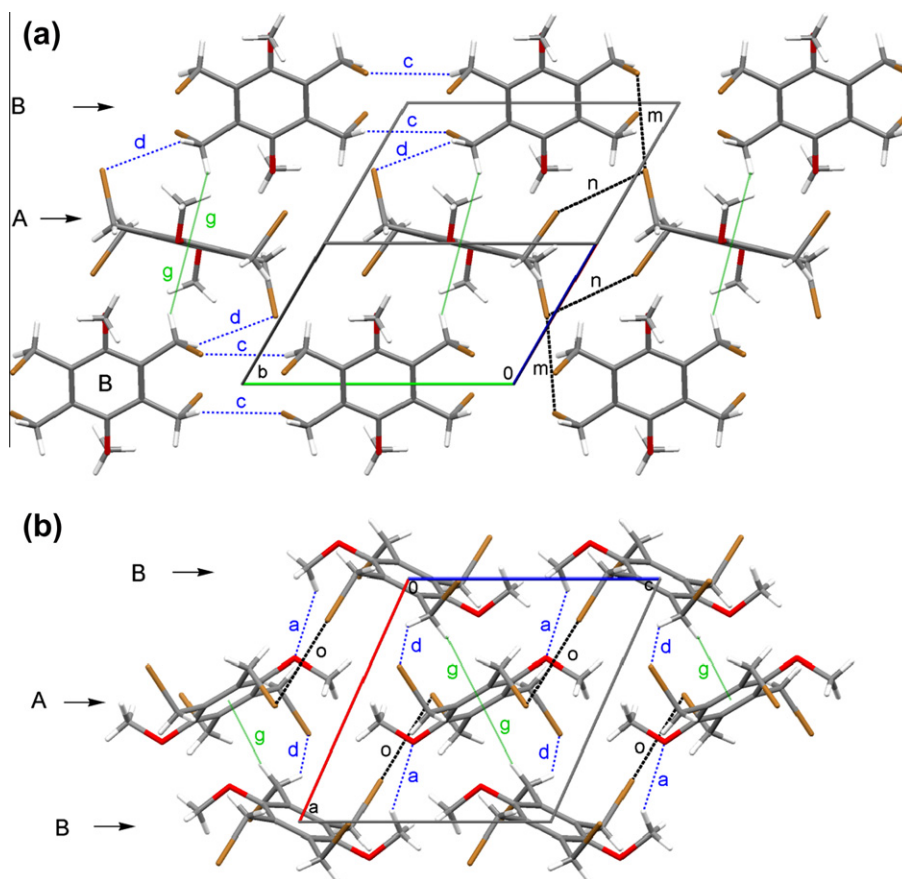


Fig. 4. Plots of  $d_{\text{norm}}$  isosurfaces of (a) two asymmetric molecules A and B of **1**; (b) molecule of **2**; (c) molecule of **3**. The position of the short C–H··· $\pi$  contact on the isosurfaces of molecules **1A** (acceptor) and **1B** (donor) are indicated with arrows.



**Fig. 5.** (a) Non-resolved fingerprint plots for two asymmetric molecules A and B of **1**, as well as for compounds **2** and **3**; (b) Fingerprint plots resolved for various modes of intermolecular interactions. The percentages show the contribution of a particular contact to the total Hirshfeld surface area of molecules. Characteristic features of the fingerprint plots are marked with arrows.



**Fig. 6.** Two views of intermolecular interactions in the crystal lattice of **1**. Dashed lines represent CH...Br (**a**, **c**, **d**; blue, shown only on the left side of the image **a**), Br...Br (**m**–**o**; thick black, shown only on the right side of the image **a**), and C–H... $\pi$  (**g**; green) contacts. Only the contacts with the distances below the sum of vdW radii of the involved atoms are shown. The contact distances are given in Tables 2–3. Rows of the two types of asymmetric molecules are labeled as “A” and “B”. (For interpretation of the references to color in this figure legend, the reader is referred to the web version of this article.)

**Table 2**  
Intermolecular hydrogen bonds for compounds **1**–**3**.<sup>a</sup>

Compound		D–H...A	DH...A (Å)	D...A (Å)	D–H...A (°)	Symmetry code
<b>1</b>	<i>a</i>	C12–H123...O1	2.61	3.368(4)	137	1 + x, y, z
	<i>b</i>	C12–H122...O1	2.87	3.738(4)	151	1 – x, 1 – y, 1 – z
	<i>c</i>	C11–H112...Br10	3.02	3.775(3)	135	2 – x, 2 – y, 2 – z
	<i>d</i>	C10–H101...Br4	3.02	3.751(3)	133	x, y, z
	<i>e</i>	C4–H41...Br5	3.11	3.789(3)	129	1 – x, 2 – y, 1 – z
	<i>f</i>	C5–H52...Br11	3.12	3.756(3)	125	x, y, –1 + z
	<i>g</i>	C10–H102...Cg <sup>b</sup>	2.60	3.492(4)	152	x, y, z, 1 – x, 1 – y, 1 – z
<b>2</b>	<i>h</i>	C7–H72...Br4	3.12	4.101(3)	172	x, –1 + y, z
	<i>i</i>	C10–H102...Br5	3.15	3.974(3)	143	2 – x, –1/2 + y, 1/2 – z
	<i>j</i>	C8–H82...Br4	3.17	3.822(3)	127	2 – x, –1/2 + y, 1/2 – z
<b>3</b>	<i>k</i>	C10–H102...O1	2.73	3.623(2)	157	–x, –y, 1 – z
	<i>l</i>	C5–H52...Br4	3.13	3.7666(16)	125	1 – x, 1 – y, 1 – z

<sup>a</sup> Only the contacts with  $\angle(\text{D–H...A}) > 120^\circ$  are included into the table.

<sup>b</sup> Cg is the centroid of the C1–3, C1<sup>1</sup>–3<sup>1</sup> ring of the compound **1**.

**Table 3**  
Bromine–bromine contacts for compounds **1**–**3**.

Compound		C–Br...Br–C	Br...Br (Å)	C–Br...Br, Br...Br–C (°)	Symmetry code
<b>1</b>	<i>m</i>	C4–Br4...Br10–C10	3.5165(7)	169.51(12), 115.47(10)	2 – x, 2 – y, 2 – z
	<i>n</i>	C4–Br4...Br5–C5	3.6472(8)	78.54(12), 150.37(13)	1 – x, 2 – y, 1 – z
	<i>o</i>	C5–Br5...Br11–C11	3.6146(8)	78.47(12), 159.07(13)	x, y, –1 + z
<b>2</b>	<i>p</i>	C4–Br4...Br4–C4	3.6638(7)	165.90(7), 100.33(7)	2 – x, 1/2 + y, 1/2 – z, 2 – x, –1/2 + y, 1/2 – z
	<i>q</i>	C5–Br5...Br5–C5	3.8530(7)	126.11(7) $\times$ 2	3 – x, 1 – y, 1 – z
<b>3</b>	<i>r</i>	C5–Br5...Br5–C5	3.5093(12)	143.95(5) $\times$ 2	1 – x, 1 – y, –z

modes of intermolecular interactions were drawn and analyzed. Unresolved fingerprint plots of the two asymmetric molecules are already remarkably different (Fig. 5a). Analysis of the fingerprint plots resolved for different modes of interactions has shown that the major difference was due to O···H and C···H short contacts (Fig. 5b). Two pointed wedges (marked with arrows, one associated with the acceptor O-atom of the molecule A, the other with the donor H-atom of the molecule B) indicate the presence of strong non-classical CH<sub>2</sub>···O hydrogen bonds. The difference between C···H-resolved fingerprint plots was especially remarkable, showing a pair of relatively extended complementary protrusions on asymmetric molecules (Fig. 5b), marked with arrows). Analysis of the molecular packing gave evidence of a relatively rare highly symmetric short C–H···π contact: an H-atom of molecule B is located directly above the middle of the benzene ring of molecule A with  $d(\text{H}\cdots\text{Cg}(B)) = 2.60 \text{ \AA}$  and  $\angle(\text{C–H}\cdots\text{Cg}(B)) = 152^\circ$ . This

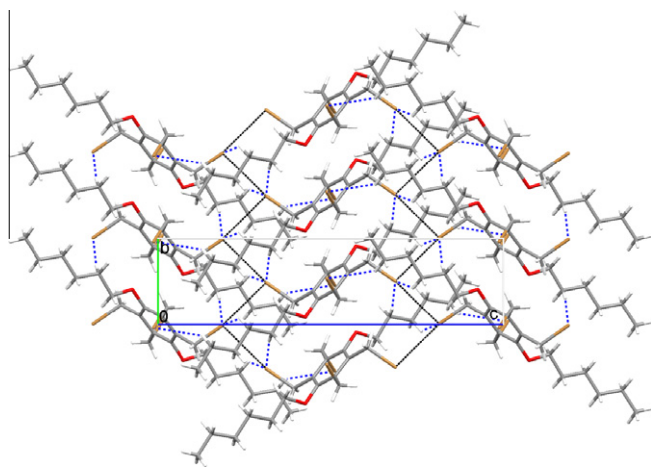


**Fig. 7.** Intermolecular interactions in the crystal lattice of **2** viewed along the *a* axis. Dashed lines represent Br···Br (thick black), and CH···Br (blue) short contacts; the latter are shown for the  $d \leq (r_{vdW} + 0.2)$  nm. The contact distances are given in Tables 2–3. (For interpretation of the references to color in this figure legend, the reader is referred to the web version of this article.)

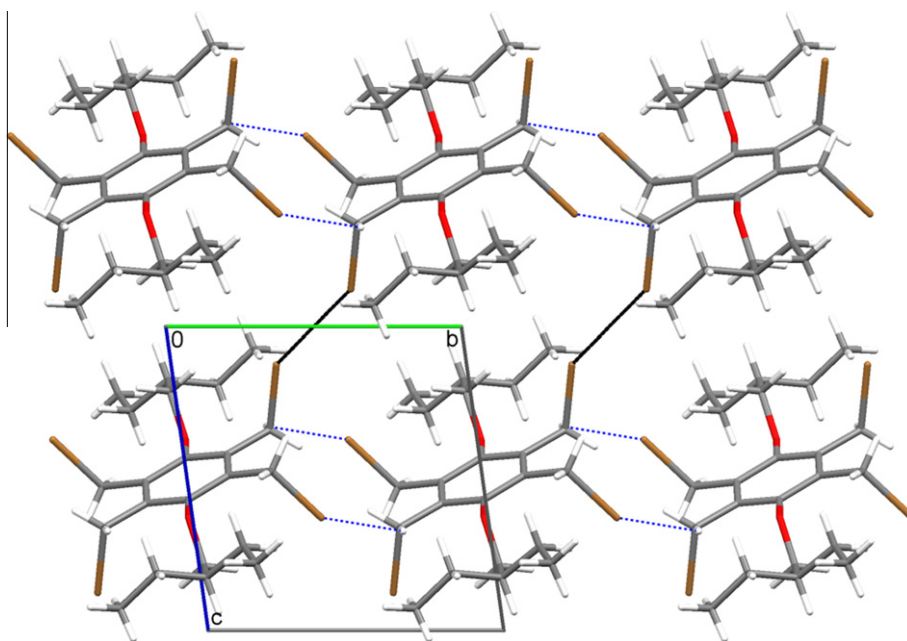


**Fig. 8.** Intermolecular interactions in the crystal lattice of **3** viewed along the *a* axis. Dashed lines represent Br···Br (thick black), and CH···Br (blue) short contacts; the latter are shown for the  $d \leq (r_{vdW} + 0.1)$  nm. The contact distances are given in Tables 2–3. (For interpretation of the references to color in this figure legend, the reader is referred to the web version of this article.)

contact is also well-distinguishable on the  $d_{norm}$  fingerprint plots of the two asymmetric molecules of **1** (Fig. 4a).

Additionally, analysis of fingerprint plots resolved for Br···Br contacts showed the presence of short and highly directional Br···Br interactions, appearing as sharp and long traces. Fingerprint plots for Br···H interactions afforded evidence for numerous C–H···Br non-classical H-bonds, which show up as two broad pointed wings. H···H interactions, although large in surface, show rather diffuse character.

In the crystal, two symmetrically non-equivalent molecules pack into infinite chains of molecules *A* and *B* (Fig. 6) along the *b* axis. The angle between the planes of the benzene rings of the individual molecules in chain *A* relative to chain *B* amounts to  $60.9(2)^\circ$ . Whereas the molecules in the chains *A* are connected by CH<sub>2</sub>···Br interactions **c**, the chains *B* are linked by Br···Br contacts **n** (Fig. 6a). Between the chains *A* and *B*, Br···Br contacts **m** and **n**, as well as CH<sub>2</sub>···O hydrogen bonds **a** and CH<sub>2</sub>···Br H-bonds **d** can be recognized. All Br···Br contacts belong to the stronger type II halogen···halogen interaction according to the classification of Desiraju et al. [30]. Several additional C–H···A (A = O or Br) contacts can be recognized slightly above the sum of the *vdW* radii of the neighboring atoms involving both bromine and oxygen as the donor atoms (for the full listing, see Tables 2 and 3). Finally, the C–H···π contact also links pairs of asymmetric molecules with each other.

The fingerprint plots of compounds **2** and **3** do not exhibit many characteristic features (Fig. 5): due to the presence of the extended alkyl chains, the  $d_{norm}$  contact areas are dominated by diffuse H···H and Br···H short contacts. On the H···H-resolved plot of **3**, one particularly short H···H contact is denoted by the two sharp spikes in the low left corner, whereas the O···H-resolved plot shows the presence of one O···H contact. Accordingly, compounds **2** (Fig. 7) and **3** (Fig. 8) only show one particularly close Br···Br contact each, and **3** has one of the side chain hydrogens contact the CH<sub>2</sub>Br hydrogens within the van der Waals distance as well (Tables 2 and 3). Several CH<sub>2</sub>···A (where A = Br, O) “borderline” [31] contacts can be recognized in both structures, although all contact distances lie slightly above the sum of the *vdW* radii.

### 3.3. OPiX calculations

The program OPiX was used in order to check whether this “classic” method of studying intermolecular interactions is corroborated by the calculated intermolecular energies, both in a simple UNI force field calculation for all compounds, and via the PIXEL method applied to a B3LYP/6-311G\* density of compound **1** (Table 4).

Listing all cohesive molecular pairs with interaction energies over 5 kJ/mol according to the UNI force field (Table 5) leads to four molecular pairs in compound **2**, and six pairs in compound **3**. Compound **1** is the most interesting, as there are two symmetry independent molecules in the asymmetric unit, and interactions can be studied between the pairs of symmetric and asymmetric molecules.

Three clear conclusions can be drawn from these tables: the first is that the PIXEL energies in general agree relatively well with the figures from the UNI force field calculations, although the latter, for **1**, has a tendency to overestimate the interaction energy with respect to the PIXEL method.

The second conclusion is that Br···Br and CH···Br interactions are by far not the most important factor in the packing of these crystal structures. The main part of the cohesive energy of the structures is due to dispersion interactions, with directional interactions playing only a minor role, especially in compounds **2** and **3**, which can be also concluded from examination of their fingerprint plots (see above).

**Table 4**  
Intermolecular interaction energies calculated for **1–3** using PIXEL method and UNI force field.

	$\Delta H$ PIXEL (B3LYP/6-311G*), kJ/mol	$\Delta H$ UNI-FF, kJ/mol
1	–225.6	–255.3
2	–	–195.0
3	–	–170.3

**Table 5**  
Cohesive molecular pairs with interaction energies over 10 kJ/mol according to PIXEL method and/or UNI force field. Numbers in bold are the totals for a particular kind of interaction.

	$\Delta H$ PIXEL, kJ/mol	$\Delta H$ UNI-FF, kJ/mol	Interactions <sup>a</sup>	Symmetry code <sup>d</sup>
1, A···A	–32.7 <sup>b</sup>	–34.3 <sup>c</sup>		
	–12.5	–11.9	–	$x, -1 + y, -1 + z$
	–12.5	–9.9	<i>n</i>	$x, -1 + y, z$
1, A···B	–120.8 <sup>b</sup>	–178.2 <sup>c</sup>		
	–38.1	–50.4	<i>b,d,g</i>	$x, y, z$
	–18.0	–20.6	<i>a,o</i>	$-1 + x, y, z$
	–8.9	–11.7	<i>m</i>	$-1 + x, -1 + y, -1 + z$
1, B···B	–35.6 <sup>b</sup>	–28.5 <sup>c</sup>		
	–14.9	–11.4	–	$x, -1 + y, -1 + z$
	–17.5	–10.1	<i>c</i>	$x, -1 + y, z$
2	–	–89.7	<i>h</i>	$x, -1 + y, z$
	–	–18.5	<i>p</i>	$x, -1/2 + y, -1/2 + z$
	–	–14.7	–	$-1 + x, -1/2 + y, -1/2 + z$
3	–	–58.8	<i>k</i>	$-1 + x, y, z$
	–	–34.0	–	$-1 + x, y, 1 + z$
	–	–26.3	–	$-1 + x, 1 + y, z$
	–	–17.3	<i>l</i>	$x, -1 + y, z$

<sup>a</sup> See Tables 2 and 3 for designation of the numbers.

<sup>b</sup> Polarization is not included in the interaction energies for molecular pairs.

<sup>c</sup> Molecular pairs with energy contributions below the cut-off implemented in OPiX could not be included into these sums.

<sup>d</sup> Symmetry codes used for OPiX calculations differ from the ones used for crystal descriptions, see Section 2.

The third observation is that for compound **1** there is a large number of intermolecular directional interactions and hydrogen bonds present in the crystal structure. The majority of them occurs between the non-symmetry-equivalent molecules and the total interaction energy between these molecular pairs is much larger than between the symmetry-equivalent molecular pairs. This leads to the conclusion that in the case of **1** the structure can trade lower  $Z'$  against a more optimized packing, which utilizes more of the functionalities present in the molecules for formation of attractive intermolecular contacts. This conclusion corresponds well to the statistical observation that the asymmetric molecular pairs rank first in the list of intermolecular interaction energies in 55–60% of the *ca.* 5000  $Z' > 1$  crystals structures investigated in a recent study [32]. Furthermore, the crystal structure of **1** contains a combination of several different directional supramolecular synthons (CH···Br and CH<sub>2</sub>···O hydrogen bonds, Br···Br and CH··· $\pi$  interactions) with their particular structural tendencies, which was shown to be a common feature for structures formed with  $Z' > 1$  [33].

The cause of such  $Z' > 1$  packing lies most likely in a discrepancy between the molecular shape and the character of intermolecular interactions. In this way, compound **1** obtains better stabilization not by using the same energetically beneficial directional interactions between two symmetry related molecules, and thus packing with  $Z' = 1$ , but rather by trading them for different interactions between symmetrically unrelated molecules, in which the same hydrogen, bromine and oxygen atoms play different roles as donors or acceptors, providing overall better stabilization.

The better stabilization of the crystal packing of **1** through numerous intermolecular contacts also corresponds well with its physical properties: compound **1** has by far the highest melting point in comparison with **2–3** and 1,2,4,5-tetrakis(bromomethyl)benzene and a noticeably lower solubility in common organic solvents, such as chloroform, benzene, or acetone.

## 4. Conclusions

As a conclusion we can state that the CH<sub>2</sub>Br groups play the most important role in the crystal packing of compound **1**. Bromomethylene groups participate in the formation of weak hydrogen bonds both as H-bond donors and acceptors, and are also involved in the formation of Br···Br contacts. The role of the O-atoms in the intermolecular packing is relatively small, since they barely participate in the formation of H-bonds. Compound **1** displays a complex network of stabilizing CH<sub>2</sub>···A, Br···Br, and CH··· $\pi$  short contacts in the crystal. The array of directional interactions interconnecting the asymmetric pairs of molecules is much more complex and more stabilizing than the one between the symmetrically equivalent ones, which leads to crystallization of **1** with higher  $Z'$ . On the other hand, the presence of the long alkyl substituents in compounds **2** and **3** inhibits close contacts of functional groups able to participate in directional interactions, preventing the formation of an extended network of CH<sub>2</sub>···A, Br···Br, and CH··· $\pi$  contacts, and as a result their packing stabilization is mainly based on van der Waals interactions. Finally, examination of Hirshfeld surfaces and fingerprint plots proved to be a useful method of analysis for the structures with  $Z' > 1$  [34], allowing handy determination of asymmetric interactions between the non-equivalent molecules.

## Supplementary material

CCDC 860468–860470 contain the supplementary crystallographic data for **1–3**. These crystallographic data can be obtained free of charge from via <http://www.ccdc.cam.ac.uk/conts/retriev>

ing.html, or from the Cambridge Crystallographic Data Centre, 12 Union Road, Cambridge CB2 1EZ, UK; fax: +44 1223 336 033.

## Acknowledgements

The X-ray diffractometer (M.Z.) was funded by NSF Grant 0087210, Ohio Board of Regents Grant CAP-491 and Youngstown State University. V.A.A. is grateful to BFK-NaWi for financial support. C.V.V. thanks Frank Blockhuys (University of Antwerp, Belgium) for the theoretical calculation on **1**, on the university's computer cluster CalcUA.

## References

- [1] (a) G.R. Desiraju, T. Steiner, *The Weak Hydrogen Bond in Structural Chemistry and Biology*, Oxford University Press, Oxford, 1999;
- (b) T. Steiner, *Angew. Chem., Int. Ed.* 41 (2002) 48–76;
- (c) G.R. Desiraju, *Chem. Commun.* (2005) 2995–3001.
- [2] (a) P. Metrangolo, G. Resnati, *Chem. Eur. J.* 7 (2001) 2511–2519;
- (b) P. Metrangolo, H. Neukirch, T. Pilati, G. Resnati, *Acc. Chem. Res.* 38 (2005) 386–395;
- (c) P. Metrangolo, F. Meyer, T. Pilati, G. Resnati, G. Terraneo, *Angew. Chem. Int. Ed.* 47 (2008) 6114–6127;
- (d) K. Rissanen, *Cryst. Eng. Comm.* 10 (2008) 1107–1113.
- [3] (a) E.A. Meyer, R.K. Castellano, F. Diederich, *Angew. Chem. Int. Ed.* 42 (2003) 1210–1250;
- (b) S. Grimme, *Angew. Chem. Int. Ed.* 47 (2008) 3430–3434;
- (c) M. Nishio, Y. Umezawa, K. Honda, S. Tsuboyama, H. Suezawa, *CrystEngComm* 11 (2009) 1757–1788;
- (d) D. Swierczynski, R. Luboradzki, G. Dolgonos, J. Lipkowski, H.-J. Schneider, *Eur. J. Org. Chem.* (2005) 1172–1177;
- (e) I. Saraogi, V.G. Vijay, S. Das, K. Sekar, T.N. Guru Row, *Cryst. Eng.* 6 (2003) 69–77.
- [4] J.D. Dunitz, A. Gavezzotti, *Chem. Soc. Rev.* 38 (2009) 2622–2633.
- [5] (a) A.D. Thomas, L.L. Miller, *J. Org. Chem.* 51 (1986) 4160–4169;
- (b) S.F. Rak, T.H. Jozefiak, L.L. Miller, *J. Org. Chem.* 55 (1990) 4794–4801;
- (c) S. Li, Z. Li, K.-I. Kanno, T. Takahashi, K. Nakajima, *Chem. – Asian J.* 4 (2009) 294–301.
- [6] (a) J. Roehrich, P. Wolf, V. Enkelmann, K. Muellen, *Angew. Chem. Int. Ed. Engl.* 27 (1988) 1377–1379;
- (b) J. Roehrich, K. Muellen, *J. Org. Chem.* 57 (1992) 2374–2379.
- [7] (a) J. Kang, G. Hilmersson, J. Santamaria, J. Rebek Jr., *J. Am. Chem. Soc.* 120 (1998) 3650–3656;
- (b) J.M. Rivera, T. Martin, J. Rebek Jr., *J. Am. Chem. Soc.* 123 (2001) 5213–5220.
- [8] (a) H. Iwamoto, N. Takahashi, T. Maeda, Y. Hidaka, Y. Fukazawa, *Tetrahedron Lett.* 46 (2005) 6839–6842;
- (b) V.A. Azov, R. Gomez, J. Stelten, *Tetrahedron* 64 (2008) 1909–1917;
- (c) M. Skibinski, R. Gomez, E. Lork, V.A. Azov, *Tetrahedron* 65 (2009) 10348–10354.
- [9] (a) J.J. McKinnon, M.A. Spackman, M.S. Mitchell, *Acta Cryst. B* 60 (2004) 627–668;
- (b) J.J. McKinnon, D. Jayatilaka, M.A. Spackman, *Chem. Commun.* (2007) 3814–3816;
- (c) M.A. Spackman, D. Jayatilaka, *CrystEngComm* 11 (2009) 19–32.
- [10] Bruker AXS Inc., APEX2, SAINT and SADABS, Madison, Wisconsin, USA, 2009.
- [11] A. Altomare, G. Cascarano, G. Giacovazzo, A. Guagliardi, M.C. Burla, G. Polidori, M. Camalli, *J. Appl. Cryst.* 27 (1994) 435.
- [12] P.W. Betteridge, J.R. Carruthers, R.I. Cooper, K. Prout, D.J. Watkin, *J. Appl. Cryst.* 36 (2003) 1487.
- [13] R.I. Cooper, A.L. Thompson, D.J. Watkin, *J. Appl. Cryst.* 43 (2010) 1100–1107.
- [14] L.J. Farrugia, *J. Appl. Cryst.* 30 (1997) 565.
- [15] (a) A.L. Spek, *J. Appl. Cryst.* 36 (2003) 7–13;
- (b) A.L. Spek, *Acta Cryst. D* 65 (2009) 148–155.
- [16] S.K. Wolff, D.J. Grimwood, J.J. McKinnon, D. Jayatilaka, M.A. Spackman, *CrystalExplorer 2.1*, University of Western Australia, Perth, 2007.
- [17] C.F. Macrae, P.R. Edgington, P. McCabe, E. Pidcock, G.P. Shields, R. Taylor, M. Towler, J. van de Streek, *J. Appl. Cryst.* 39 (2006) 453–457.
- [18] (a) M.A. Spackman, P.G. Byrom, *Chem. Phys. Lett.* 267 (1997) 215–220;
- (b) J.J. McKinnon, A.S. Mitchell, M.A. Spackman, *Chem. Eur. J.* 4 (1998) 2136–2141.
- [19] M.A. Spackman, J.J. McKinnon, *CrystEngComm* 4 (2002) 378–392.
- [20] (a) R.M. Ibberson, S. Parsons, D.R. Allan, A.M.T. Bell, *Acta Cryst. B* 64 (2008) 573–582;
- (b) S. Roy, A.J. Matzger, *Angew. Chem. Int. Ed.* 48 (2009) 8505–8508;
- (c) D. Das, E. Engel, L.J. Barbour, *Chem. Commun.* 46 (2010) 1676–1678;
- (d) M. Bujak, A. Katrusiak, *CrystEngComm* 12 (2010) 1263–1268.
- [21] (a) T.E. Clark, M. Makha, A.N. Sobolev, C.L. Raston, *Cryst. Growth Des.* 8 (2008) 890–896;
- (b) D.S. Yufit, J.A.K. Howard, *CrystEngComm* 12 (2010) 737–741.
- [22] (a) M. Bujak, K. Dziubek, A. Katrusiak, *Acta Cryst. B* 63 (2007) 124–131;
- (b) R. Gajda, A. Katrusiak, *Cryst. Growth Des.* 8 (2008) 211–214.
- [23] M.J. Frisch et al., *Gaussian 03*, Gaussian, Inc., Wallingford, CT, USA, 2004.
- [24] A. Gavezzotti, *OpiX*, A Computer Program Package for Calculation of Intermolecular and Crystal Energies, University of Milano, Milan, Italy, 2003.
- [25] A. Gavezzotti, *Struct. Chem.* 220 (2005) 499–510.
- [26] P. Marsau, *Acta Crystallogr.* 18 (1965) 851–854.
- [27] (a) P.G. Jones, P. Kuś, *Z. Naturforsch.* 62b (2007) 725–731;
- (b) Z.-G. Wang, Y.-Z. Wang, N.-F. She, M. Gao, *Acta Cryst. E* 62 (2006) 5106–5107.
- [28] C.B. Aakeröy, T.A. Evans, K.R. Seddon, I. Pálinkó, *New. J. Chem.* (1999) 145–152.
- [29] A. Bondi, *J. Phys. Chem.* 68 (1964) 441–451.
- [30] V.R. Pedireddi, D.S. Reddy, B.S. Goud, D.C. Craig, A.D. Rae, G.R. Desiraju, *J. Chem. Soc., Perkin Trans. 2* (1994) 2353–2360.
- [31] (a) W.-W. du Mont, M. Bätcher, C. Daniliuc, F.A. Devillanova, C. Druckenbrodt, J. Jeske, P.G. Jones, V. Lippolis, F. Ruthe, E. Seppälä, *Eur. J. Inorg. Chem.* (2008) 4562–4577;
- (b) P.G. Jones, P. Kuś, *Z. Naturforsch.* 65b (2010) 433–444.
- [32] A. Gavezzotti, *CrystEngComm* 10 (2008) 389–398.
- [33] K.M. Anderson, A.E. Goeta, J.W. Steed, *Cryst. Growth Des.* 8 (2008) 2517–2524.
- [34] For other examples of Hirshfeld surface analysis of structures with  $Z' > 1$ , see: (a) B. Chattopadhyay, H.P. Hemantha, N. Narendra, V.V. Sureshbabu, J.E. Warren, M. Helliwell, A.K. Mukherjee, M. Mukherjee, *Cryst. Growth Des.* 10 (2010) 2239–2246;
- (b) K.M. Anderson, S.E. Tallentire, M.R. Probert, A.E. Goeta, B.G. Mendis, J.W. Steed, *Cryst. Growth Des.* 11 (2011) 820–826.